

# Coupling measurements for the 125 GeV Higgs Boson in the fermion decay channels with the ATLAS detector

---

**Duc Bao Ta, on behalf of the ATLAS collaboration**

*University of Freiburg (Germany)*

*E-mail: [xiedebao@googlemail.com](mailto:xiedebao@googlemail.com)*

Detailed measurements of the properties of the 125 GeV Higgs boson are fundamental for the understanding of the mechanism responsible for the electroweak symmetry breaking. Measurements of the Higgs boson in fermion final states allow to study the Yukawa couplings of the Higgs boson through the decay mode and the gauge couplings of the Higgs boson through the production mode. This talk summarizes the measurements of the 125 GeV Higgs boson in decays involving  $b$  quarks,  $\tau$  leptons and muons with the ATLAS experiment at the LHC.

*XXV International Workshop on Deep-Inelastic Scattering and Related Subjects*  
*3-7 April 2017*  
*University of Birmingham, UK*



## 1. Introduction

In the Higgs-mechanism of the Standard Model (SM) the mass generation mechanism for fermions is realised by Yukawa interactions [1–6]. The coupling strength is predicted to be proportional to the fermion mass. To test the prediction and to confirm the Yukawa sector of the Higgs-boson couplings, measurements of the Higgs-boson production and decay into fermions have been performed with ATLAS experiment [7] at the LHC. This paper summarizes the results on the decay to  $b$  quarks, to  $\tau$  leptons and to muons.

The Higgs-boson production at the LHC is mainly through the three following bosonic modes: the gluon fusion (ggF), the vector-boson fusion (VBF) and the associated production mode (VH). In the ggF production mode the gluons couple through a fermion loop (mainly top quarks) to the Higgs boson. It has the largest contribution and it is experimentally accessible through the accessible Higgs-decay modes such as  $H \rightarrow \gamma\gamma, WW(\rightarrow \ell\nu\ell'\nu'), ZZ(\rightarrow 4\ell), \tau\tau, \mu\mu$ . This is helpful for suppression of multi-jet background and the leptons can be used to trigger the event. Usually an additional jet is required in the signature and this leads to a boost of the Higgs boson. The VBF mode has an exploitable topology for the background suppression. The Higgs boson is produced by two vector bosons that have been radiated off the initial partons. The outgoing quarks still carry a large momentum in forward direction, so that two jets at large absolute pseudorapidities can be found. Also the interaction between the two partons is QCD-colourless, so that between the two largely separated jets no other objects than the Higgs-boson decay products can be found. The Higgs-boson production can also be accompanied by a vector boson. The VH production mode has the smallest contribution among the three main modes. The vector boson can be used for additional background suppression and triggering of the event by using the leptonic decay modes of the vector boson. This leads to leptons or missing transverse energy ( $E_T^{\text{miss}}$ ) that can be used for triggering of the events and background suppression.

The results of the measurements are expressed in terms of the signal strength  $\mu = \frac{\sigma \times \text{BR}}{(\sigma \times \text{BR})_{\text{SM}}}$  where  $\sigma \times \text{BR}$  is the measured and  $(\sigma \times \text{BR})_{\text{SM}}$  is the predicted production cross-section in the SM. All results are expressed at a Higgs-boson mass of  $m_H = 125$  GeV, except for the Run-1  $H \rightarrow \tau\tau$  which uses  $m_H = 125.36$  GeV.

The cross section of the gluon-fusion process is taken from a calculation at next-to-next-to-leading-order (NNLO) in QCD, including soft-gluon resummation up to next-to-next-to-leading logarithm terms (NNLL). Next-to-leading order (NLO) electroweak (EW) corrections are also included. For the latest 13 TeV  $H \rightarrow \mu\mu$  analysis it is even calculated at next-to-next-to-next-to-leading-order (N3LO) QCD [8] and NLO electroweak accuracies [9, 10]. The vector-boson fusion cross section has been calculated with full NLO QCD and EW corrections with an approximate NNLO QCD correction applied. The VH production cross section has been calculated at NNLO in QCD, with NLO EW radiative corrections applied. A summary of the state-of-the-art calculations and references are summarized in Reference [11].

The measurements presented here have been performed either using the whole Run-1 dataset (corresponding to an integrated luminosity of  $\mathcal{L} = 4.5 \text{ fb}^{-1} + 20.3 \text{ fb}^{-1}$  for 7 TeV and 8 TeV, resp.) or only the data taken at a centre-of-mass energy of 8 TeV ( $\mathcal{L} = 20.3 \text{ fb}^{-1}$ ) or the first data taken at 13 TeV in Run-2 of the LHC ( $\mathcal{L} = 13.2 \text{ fb}^{-1}$ ,  $\mathcal{L} = 36.1 \text{ fb}^{-1}$  for  $H \rightarrow \mu\mu$ ).

## 2. Measurements of $H \rightarrow \tau\tau$

The decay into a pair of  $\tau$  leptons is the largest leptonic decay mode (branching ratio  $\sim 6.3\%$ ) and the events in the signal selection are dominated by background events from  $Z$ -boson production or multi-jet events. To maximize the acceptance of signal events also hadronically decaying  $\tau$  leptons are considered by using dedicated  $\tau$  lepton trigger and  $\tau$  lepton identification algorithms.

The measurement of the  $H \rightarrow \tau\tau$  process uses the full Run-1 dataset [12]. Three orthogonal selection channels according to the decay modes of the  $\tau$  lepton are used. These are denoted with  $\tau_{\text{lep}}\tau_{\text{lep}}$ ,  $\tau_{\text{lep}}\tau_{\text{had}}$  and  $\tau_{\text{had}}\tau_{\text{had}}$ , depending on the leptonic ( $\tau_{\text{lep}}$ ) or hadronic decay mode ( $\tau_{\text{had}}$ ). The  $\tau$  leptons are identified with  $\tau$  identification algorithms that use multivariate techniques (MVA).

The event selection has optimized selection categories for ggF and VBF production mode to maximize the sensitivity. The signal strength is determined from a maximum-likelihood fit of multivariate discriminants for each category, each signal and background control-region, each channel and each centre-of-mass energy. The multivariate discriminants are obtained from boosted decision trees (BDT). The most powerful discriminant between signal and background is the reconstructed Higgs-boson mass (MMC) [13]. The missing kinematic information on the two-four neutrinos is recovered by using the matrix element probability of a certain kinematic configuration of the event. This distribution is shown in Figure 1 for the full Run-1 data with the best fit signal strength.

The measured signal strength is  $\mu = 1.43^{+0.27}_{-0.26}(\text{stat.})^{+0.32}_{-0.25}(\text{syst.}) \pm 0.09(\text{theory syst.})$  (using a Higgs-boson mass of  $m_H = 125.36$  GeV), which is consistent with the predicted coupling strength. The (expected) significance of the measurement is 4.5 (3.4) standard deviations which provides evidence of the  $H \rightarrow \tau\tau$  decay. The combination [14] with the Run-1 result from CMS yields evidence for the decay  $H \rightarrow \tau\tau$  with a measured significance of 5.5 standard deviations.

The analysis of the associated production  $VH$  with  $H \rightarrow \tau\tau$  uses the full 8 TeV dataset [15]. Although the measurement of the associated production mode has a smaller cross section, the leptonic decay modes of the associated boson can help the suppression of background and give additional objects for triggering the event. This is especially useful when considering the  $\tau$  lepton final states with at least one hadronically decaying  $\tau$  lepton.

In total four channels are considered where the associated boson is a  $W$  boson or a  $Z$  boson and the Higgs bosons decays into the  $\tau_{\text{lep}}\tau_{\text{had}}$  or  $\tau_{\text{had}}\tau_{\text{had}}$  final state. For each channel a dedicated selection exploits the unique number of leptons and  $\tau$  leptons and their charge combinations.

For the signal extraction a mass discriminant is used. In the  $ZH$  channels the MMC is used with the lepton that is not used in the  $Z$  boson reconstruction and the  $E_T^{\text{miss}}$  is expected to come entirely from the  $\tau$  lepton decays. For the  $WH$  channels due to the additional presence of a neutrino,  $M_{2T}$  is used, which is an event-by-event lower bound on the mass of the  $\tau\tau$  system [16].

The combined result for the measured signal strength is  $\mu = 2.3 \pm 1.6$  and a corresponding limit at 95% CL of  $\mu < 5.6$  at  $m_H = 125$  GeV ( $\mu < 3.5$  expected, if no signal is assumed and  $\mu < 3.7$  if signal is included).

## 3. Measurements of $H \rightarrow \mu\mu$

The smallest branching ratio considered here is the decay fraction into muons with a branching ratio of  $\sim 0.022\%$ . Although the coupling is extremely small when compared to the other decay

modes, the experimental signature is very clean and the Higgs-boson mass can be reconstructed with excellent mass resolution.

The search for the dimuon decay of the Higgs boson (with  $\mathcal{L} = 36.1 \text{ fb}^{-1}$  of the Run-2 dataset) has optimised selections for the VBF and the ggF production mode [17]. For this measurement the VBF category is now selected with a BDT discriminator. Events are preselected with a veto on events that contain  $b$ -tagged jets. Then two VBF categories are formed by two signal-like regions of the BDT score. Events that do not fall into the two categories are then assigned to six ggF categories. These are formed according to the  $p_T$  of the dimuon system and the  $|\eta|$  of the muons. From the eight total event categories, the most sensitive category is one of the VBF categories.

A simultaneous fit of the invariant dimuon distribution in all eight categories yield a signal strength of  $\mu = -0.07 \pm 1.5$  with a 95% CL limit of  $\mu < 3.0$  (3.1 expected). The data distribution and the fit in the most sensitive signal VBF region can be seen in Figure 2. The analysis combined the result with the previous analysis using only the Run-1 data to give the most stringent limit on the signal strength for  $H \rightarrow \mu\mu$  from ATLAS of  $\mu < 2.8$  (2.9 expected, measured  $\mu = -0.13 \pm 1.4$ ).

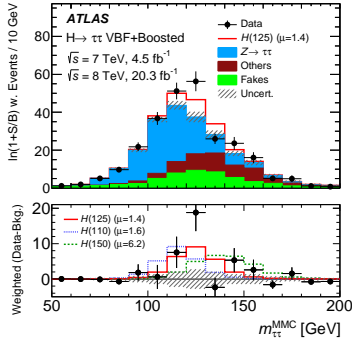


Figure 1: Reconstructed MMC distribution with the observed signal strength after the fit for the  $H \rightarrow \tau\tau$  analysis [12].

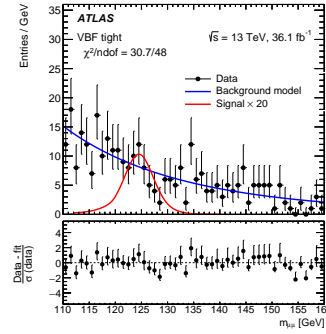


Figure 2: Invariant dimuon mass distribution and the fit result in the most sensitive VBF category for the  $H \rightarrow \mu\mu$  analysis [17].

#### 4. Measurements of $H \rightarrow b\bar{b}$

The decay into a pair of  $b$  quarks has the largest branching ratio of  $\sim 58\%$ , however the events after the selection are dominated by events with  $b$  jets from top-quark pair-production or multi-jet events with heavy quarks, that have a larger cross section. Another experimental challenge is to have a high efficiency and purity for the tagging of jets that originate from  $b$  quarks ( $b$  tagging) at reconstruction level or already at the trigger level. The measurement of the  $H \rightarrow b\bar{b}$  has been performed in three production modes, VBF production of the Higgs boson, VBF production with an associated photon and in the  $VH$  production mode.

The measurement in the VBF production mode is using the full 8 TeV dataset [18]. The selection is based on a trigger signature with one or more  $b$ -tagged jets at trigger level and the requirement of four jets ordered in  $\eta$ . The jets with the largest distance in  $\eta$  are labelled as the VBF jets, whereas the central jets are assigned to the Higgs boson and thus are required to be  $b$ -tagged.

A multivariate selection with a BDT is used to enhance the signal selection and split the events into four categories according to the BDT score. The signal strength is determined by a simultane-

ous fit to the invariant mass distribution of the  $b\bar{b}$  pair in all four categories:  $\mu = -0.8 \pm 2.3$  with a 95% CL limit of  $\mu < 4.4$  (5.4 exp.).

The signal-to-background ratio can be enhanced much more by requiring an additional high- $p_T$  photon in the final state, although the expected cross section is reduced compared to the inclusive VBF cross-section [19]. The photon provides an additional signature for triggering the event. The background is suppressed by two effects: the gluon-initiated background component of the non-resonant  $b\bar{b}\gamma jj$  background is suppressed and the destructive interference between diagrams with the hard central photon emitted from the initial-state and final-state quark lead to a further reduction of the background.

In this analysis [20] with the first Run-2 dataset four jets are required with the two central jets being  $b$ -tagged in addition. Again a BDT is used to separate signal and background and the signal is extracted from a fit to the  $m_{b\bar{b}}$  distribution in three signal categories that are formed by different ranges in the BDT score. The signal strength yields  $\mu = -3.9^{+2.8}_{-2.7}$  with a 95% CL limit of  $\mu < 4.0$  (6.0 exp.). The expected significance is worse than the VBF result, but studies have shown that it is expected to reach similar sensitivities with  $100\text{fb}^{-1}$  [19].

The analysis in the  $VH$  production channel has the best sensitivity for the  $H \rightarrow b\bar{b}$  production so far [21]. This analysis is also using the first Run-2 dataset. The event categorisation which helps to maximize the sensitivity is applied to events with two  $b$ -tagged jets. The categories are formed by the number of leptons (zero, one or two), the number of jets (zero and one, exclusive or inclusive for two-lepton events). For the event category with two leptons additional subcategories are separated by the reconstructed transverse mass of the vector boson.

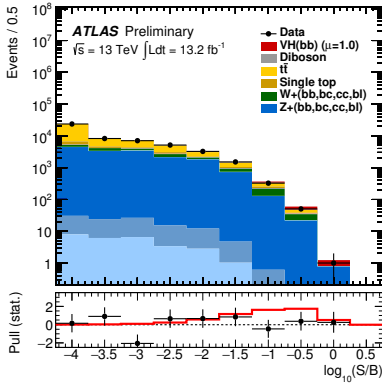


Figure 3: Event yields as a function of  $\log(S/B)$ . The final-discriminant bins in all signal regions are combined into bins of  $\log(S/B)$  for the  $VH, H \rightarrow b\bar{b}$  analysis [21].

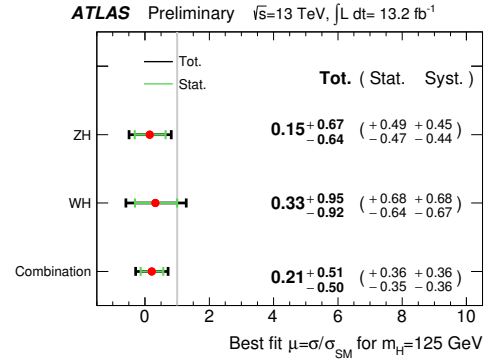


Figure 4: Breakdown of the signal strength result into the channels  $ZH$  and  $WH$  for the  $VH, H \rightarrow b\bar{b}$  analysis [21].

In each category a BDT is used as the discriminating distribution. The combined event yields as a function of  $\log(S/B)$  (signal over background) is shown in Figure 3. The simultaneous fit in all signal categories yields a signal strength of  $\mu = 0.21^{+0.36}_{-0.35}$  (stat.)  $\pm 0.36$  (syst.). This corresponds to a significance of 0.42 standard deviations (1.94 expected). A detailed break down into the two channels  $ZH$  and  $WH$  is shown in Figure 4. The observed limit is  $\mu < 1.2$  at 95% CL with an expected limit, in the absence of signal, of  $\mu < 1.0^{+0.4}_{-0.3}$ .

## 5. Summary

The latest ATLAS measurements of the Higgs boson in fermion final states ( $b$  quarks,  $\tau$  leptons and muons) that allow to study the Yukawa couplings of the Higgs boson through the decay mode have been summarized in this paper. From the measurements there is observation for the coupling to the  $\tau$  leptons (ATLAS and CMS combined) which will allow the Run-2 measurements to probe the coupling in more detail. Despite the tiny branching ratio of the  $H \rightarrow \mu\mu$  decay, limits up to  $3\times$  the SM cross section have been achieved so far. The coupling to the  $b$  quarks has not been established, yet, but already with the first Run-2 data analysis the sensitivity has been improved. A further increase is expected with the increasing amount of new data for Run-2 which is expected to at least double this year.

## References

- [1] F. Englert and R. Brout, *Phys. Rev. Lett.* **13** (1964) 321–323.
- [2] P. W. Higgs, *Phys. Rev. Lett.* **13** (1964) 508–509.
- [3] P. W. Higgs, *Phys. Lett.* **12** (1964) 132–133.
- [4] P. W. Higgs, *Phys. Rev.* **145** (1966) 1156–1163.
- [5] G. S. Guralnik, C. R. Hagen, and T. W. B. Kibble, *Phys. Rev. Lett.* **13** (1964) 585–587.
- [6] S. Weinberg, *Phys. Rev. Lett.* **19** (1967) 1264.
- [7] ATLAS Collaboration, *JINST* **3** (2008) S08003.
- [8] C. Anastasiou, C. Duhr, F. Dulat, E. Furlan, T. Gehrmann, F. Herzog, A. Lazopoulos, and B. Mistlberger, *JHEP* **05** (2016) 058, [arXiv:1602.00695](https://arxiv.org/abs/1602.00695) [hep-ph].
- [9] U. Aglietti et al., *Phys. Lett. B* **595** (2004) 432, [arXiv:hep-ph/0404071](https://arxiv.org/abs/hep-ph/0404071) [hep-ph].
- [10] S. Actis et al., *Phys. Lett. B* **670** (2008) 12, [arXiv:0809.1301](https://arxiv.org/abs/0809.1301) [hep-ph].
- [11] LHC Higgs Cross Section Working Group Collaboration, J. R. Andersen et al., [arXiv:1307.1347](https://arxiv.org/abs/1307.1347) [hep-ph].
- [12] ATLAS Collaboration, *JHEP* **04** (2015) 117, [arXiv:1501.04943](https://arxiv.org/abs/1501.04943) [hep-ex].
- [13] A. Elagin et al., *Nucl. Instrum. Meth. A* **654** (2011) 481, [arXiv:1012.4686](https://arxiv.org/abs/1012.4686) [hep-ex].
- [14] ATLAS and CMS Collaborations, *JHEP* **08** (2016) 045, [arXiv:1606.02266](https://arxiv.org/abs/1606.02266) [hep-ex].
- [15] ATLAS Collaboration, *Phys. Rev. D* **93** no. 9, (2016) 092005, [arXiv:1511.08352](https://arxiv.org/abs/1511.08352) [hep-ex].
- [16] A. J. Barr, T. J. Khoo, P. Konar, K. Kong, C. G. Lester, K. T. Matchev, and M. Park, *Phys. Rev. D* **84** (2011) 095031.
- [17] ATLAS Collaboration, ATLAS-CONF-2016-041, <https://cds.cern.ch/record/2206079>, 2016.
- [18] ATLAS Collaboration, *JHEP* **11** (2016) 112, [arXiv:1606.02181](https://arxiv.org/abs/1606.02181) [hep-ex].
- [19] E. Gabrielli, F. Maltoni, B. Mele, M. Moretti, F. Piccinini, and R. Pittau, *Nucl. Phys. B* **781** (2007) 64–84, [arXiv:hep-ph/0702119](https://arxiv.org/abs/hep-ph/0702119) [HEP-PH].
- [20] ATLAS Collaboration, ATLAS-CONF-2016-063, <https://cds.cern.ch/record/2206201>, 2016.
- [21] ATLAS Collaboration, ATLAS-CONF-2016-091, <https://cds.cern.ch/record/2206813>, 2016.